BMC Cancer

RESEARCH

Open Access

Tumor immune microenvironment in adenoid cystic carcinoma of the lacrimal gland: relationship with histopathology and prognosis

Yi Zhang[1,2,3†], Zhipeng Guo[4†], Jie Sun[1,2,3†], Yingwen Bi[5], Rongrong Cai[5], Rui Zhang[1,2,3], Hui Ren[1,2,3], Jiang Qian[1,2,3*] and Fengxi Meng[1,2,3*]

Abstract

Purpose To quantitatively investigate the pathological subtypes of lacrimal gland adenoid cystic carcinoma (LGACCs), the tumor immune microenvironment in each pathological subtype, and the relation to survival.

Methods In this retrospective study, the tumor subtype was determined by H&E staining. Multiplex immunochemistry was performed to define specific immune cells. The tumor immune microenvironment (TIME) was sketched by sequential image scanning and reconstructed by a cytometry platform.

Results Eighteen patients with adequate paraffin blocks diagnosed with LGACC from 2012 to 2021 were included in this study. Thirteen patients out of the eighteen patients (72.2%)showed a mixture of different pathological subtypes. Each pathological subtype took different percentages on different tumors. The cribriform was the most common subtype, taking an overall percentage of 39%. The rest of the pathological subtypes were tubular (19%), basaloid (17%), cribriform and tubular mixture (C+T) 14%. The sclerosing and comedocarcinomic subtypes were the least seen in LGACC, taking a percentage of 11% altogether. Patients with cribriform dominant component had better overall survival than the non-cribriform dominant patients. Patients with basaloid dominant component had worse clinical outcomes than the non-basaloid dominant ones. The TIME showed high immunogenicity in the tumor margin but declined in the tumor areas. Pathological subtypes rather than individual differences determined the TIME phenotype. The cribriform subtype possessed more immune cell infiltration than other pathological subtypes.

Conclusions LGACC is composed of multiple pathological subtypes. Each pathological subtype takes different percentages on different tumors, which is related to the prognosis. TIME pattern in LGACC varies among different pathological subtypes, which could indicate novel strategies in immunotherapy.

†Yi Zhang, Zhipeng Guo and Jie Sun contributed equally to this work.

*Correspondence:
Jiang Qian
qianjiang@fudan.edu.cn
Fengxi Meng
mfx.2000@163.com

Full list of author information is available at the end of the article

Keywords Lacrimal gland adenoid cystic carcinoma, Tumor immune microenvironment, Pathological subtype, Survival, Immunotherapy

Introduction

Adenoid cystic carcinoma is a rare but aggressive disease arising from the major salivary glands. The lacrimal gland adenoid cystic carcinoma (LGACC) is the most common type of epithelial lacrimal gland malignancies [1–5]. The tumor is notorious for its aggressive biological behavior and poor prognosis despite multimodal treatments. Adenoid cystic carcinoma in salivary glands and lacrimal glands showed morphologic and embryologic similarities [6], therefore sharing the same histopathological classification. In previous studies, LGACC were divided into five histopathological subtypes: cribriform (Swiss cheese), tubular (ductal), basaloid (solid), sclerosing, and comedocarcinomas pattern [7–10]. The histopathological patterns were believed to be related to prognosis. The presence of the solid pattern was proven to be associated with poor prognosis both in the lacrimal gland and salivary gland [7–9, 11]. Other clinicopathological risk factors related to poor prognosis include high-grade transformation, perineural invasion, vascular dissemination, nuclear atypia and MYB rearrangement [5, 7–9, 12]. However, the mechanism of the relationship between the histopathological change and clinical outcome remains unclear.

The tumor immune microenvironment (TIME) plays a critical role in the prognosis of tumors and has been extensively investigated in the past few decades. The immune system is able to eliminate tumor cells through the cancer-immune cycle [13, 14]. However, this nature biological process sometimes fails because tumors could re-shape the TIME gradually into an immunosuppressive state to support the survival of tumor cells. The delicate balance between pro- and anti-tumor inflammatory mediators plays a key role to determine tumor progression. Multiple mechanisms have been proved that tumors evolve to evade immune surveillance [14–18]. The complex immune cells participate in the tumor initiation and progression. The profile of TIME has been proven to be linked to the tumor prognosis. For example, the infiltration of myeloid-derived suppressor cells (MDSC) and tumor-associated macrophages favor tumor growth, while the cytotoxic lymphocytes provide an anti-tumor environment and indicate a better prognosis. Most studies focusing on the immune contexture were performed on salivary ACC and indicated that this tumor may exhibit low immunogenicity [11, 19–24]. However, the deep profiling of TIME based on single-cell information is lacking. Here, we retrospectively analyzed eighteen patients with a whole view of the pathological subtypes and long-term clinical follow-up outcomes. We investigated the TIME in LGACC by multiplex immunohistochemistry and revealed the immune contexture among different pathological subtypes.

Materials and methods

Patient data and tumor material

This retrospective study was carried out in the Eye and ENT Hospital of Fudan University and approved by the ethics committee of this affiliation. The clinical and research conducts adhered to the tenets of the Declaration of Helsinki. All the patients in this study have signed informed consent of clinical data investigation for research purposes. Eighteen patients with adequate paraffin blocks diagnosed with LGACC from 2012 to 2021 were included in this study. The tumor stage was classified according to the 5th edition of the WHO classification on head and neck tumors.

The pathological subtypes were determined according to previous studies on LGACC [8, 9] and evaluated separately by two experienced pathologists. The region with nuclei were processed and calculated by ImageJ. Three slides of 10 μm of each FFPE tumor block for multiplex immunochemistry were randomly picked.

To investigate the pathologic constitution of LGACC, we randomly examined three tumor sections in each of the eighteen patients. According to previous studies, LGACC was traditionally defined as five pathological patterns: cribriform/swiss cheese, tubular/ductal, basaloid/solid, sclerosing, and comedocarcinoma patterns.

Multiplex immunochemistry

The multiplex immunochemistry was conducted following the procedure developed by Tsujikawa et al. [25]. To describe the immune cell infiltration in different pathological patterns of LGACC, we chose leukocyte common antigen CD45 (BD, H130) as a preliminary marker. To identify different immune cell subtypes, a combination of biomarkers were applied for the definition, following the previous study [25]. Other primary antibodies of included in this study were (indicated as brand and clone): CD68 (Abcam, PG-M1), PD-1 (Abcam, NAT 105), CD163 (Invitrogen, 10D6), CD45 (BD, H130), Foxp3 (eBioscience, 236 A/E7), CD4 (Invitrogen, 4B12), CD8 (eBioscience, C8/144b), Csf1R (Abcam, SP211), CD3 (Thermo science, Sp7), CD56 (Invitrogen, 123C3). Sequential immunohistochemistry of ten biomarkers was conducted on each one of the tissue sections. Visualization was achieved by alcohol-soluble peroxidase substrate 3-amino-9-ethylcarbazole (AEC). Hematoxylin

(S3301, Dako) was also conducted after the deparaffinization of the FFPE slides.

Image acquisition and processing

Each round of staining was scanned and saved on the whole slide with NanoZommer S60. Chromogen stripping was confirmed by IHC negative control slides. After the ten rounds, the digital process using CellProfiler software and ImageJ pipelines [25] was conducted following the previous protocol with image preprocessing, visualization, and quantitative image analysis. All pipelines and related manuals are available at https://github.com/multiplexIHC/cppipe. FCS Express 7 Image Cytometry (De Novo Software) was applied for the pixel intensity and measurements to generate a numerical percentage of the positive immunostaining.

Statistics and survival analysis

The percentages of pathological subtypes were analyzed using descriptive statistics. Data were presented as Mean ± SEM. Overall survival was calculated with Kaplan-Meier survival analysis and log-rank tests. SPSS statistics (version 19) was used to assist with statistical analysis.

Result

Histopathological pattern constitution of LGACC

Eighteen LGACC patients with adequate paraffin blocks diagnosed from 2012 to 2021 were included in this study. The clinical and demographic characteristics of all the enrolled patients are described in Table 1.

Consistent with the traditional pathological classifications on LGACC, all the five pathological patterns (cribriform/swiss cheese, tubular/ductal, basaloid/solid, sclerosing, and comedocarcinoma patterns) were observed in our study (Fig. 1). We also noticed that in some areas, the cribriform and tubular patterns were intermixed with each other (Fig. 1E), and we defined these areas as "C + T pattern." It was typical that in one tumor, two or more components could be simultaneously observed. To further investigate the percentages of the specific patterns in each tumor, we used ImageJ software to delineate the borders of tumor cell areas (Supplementary Fig. 1). The matrix areas were not counted. As demonstrated in Fig. 2A and B, the cribriform was the most common type, taking an overall percentage of 39%. The tubular pattern was the second common phenotype, taking a percentage of 19%. The basaloid pattern took 17%, and the C + T pattern took 14%. The sclerosing and comedocarcinoma patterns were rare, taking 11% altogether. The heatmap in Fig. 2A displayed the pathological phenotype in each tumor. The numbers below represented patient numbers on Fig. 2A. Most tumors showed a mixture of two or three types, with different percentages. Due to a relatively smaller volume of the orbit compared to other parts of the body, most lacrimal gland tumors were usually detected at early T stages due to eye swollenness. First, we compared the patients diagnosed at T4 stages (patient number 1, 8, 10 and 11 and the other 14 patients with T2 stages established in Table 1). We did find significant differences in the survival curve between the T2 and T4 (Fig. 2C), as a commonly accepted key survival factor. Since 14 out of the 18 patients (77.8%) in

Table 1 The clinical and demographic characteristics of 18 LGACC

Case No.	Gender/Age	TNM	Eye	PNI	Treatment	Follow-up
1	F/48	T4a	OD	Y	Globe-sparing resection (bone removal), radiotherapy	NOD
2	F/40	T2a	OD	N	Globe-sparing resection, radiotherapy	DM, TRD (20)
3	M/58	T2c	OD	Y	Orbital exenteration, radiotherapy	NED
4	M/55	T2c	OD	N	Globe-sparing resection (bone removal), radiotherapy	DM, TRD (70)
5	M/25	T2c	OS	Y	Globe-sparing resection	NDA
6	F/51	T2c	OS	N	Globe-sparing resection, Orbital exenteration, Proton	LR, DM, TRD (102)
7	M/65	T2c	OS	Y	Orbital exenteration, radiotherapy	DM, TRD (20)
8	M/41	T4c	OS	Y	Globe-sparing resection (bone removal), radiotherapy	NED
9	M/51	T2c	OS	Y	Globe-sparing resection (bone removal), radiotherapy	NED
10	F/73	T4c	OS	Y	Orbital exenteration, radiotherapy	NED
11	M/45	T4c	OD	Y	Globe-sparing resection (bone removal), radiotherapy	DM, TRD (30)
12	M/57	T2c	OD	Y	Globe-sparing resection	NED
13	M/51	T2b	OD	Y	Globe-sparing resection (bone removal), radiotherapy	NED
14	F/70	T2c	OD	Y	Globe-sparing resection	DM, TRD (18)
15	F/55	T2c	OD	Y	Orbital exenteration, radiotherapy	DM, TRD (50)
16	F/48	T2b	OD	N	Orbital exenteration, Proton	NED
17	F/30	T2b	OD	N	Globe-sparing resection (bone removal), radiotherapy	NED
18	F/26	T2c	OS	Y	Globe-sparing resection, Orbital exenteration, radiotherapy	NED

DOD: die of other disease; DM: distant metastases; LR: local recurrence; NED: no evidence of disease; TRD: tumor-related death

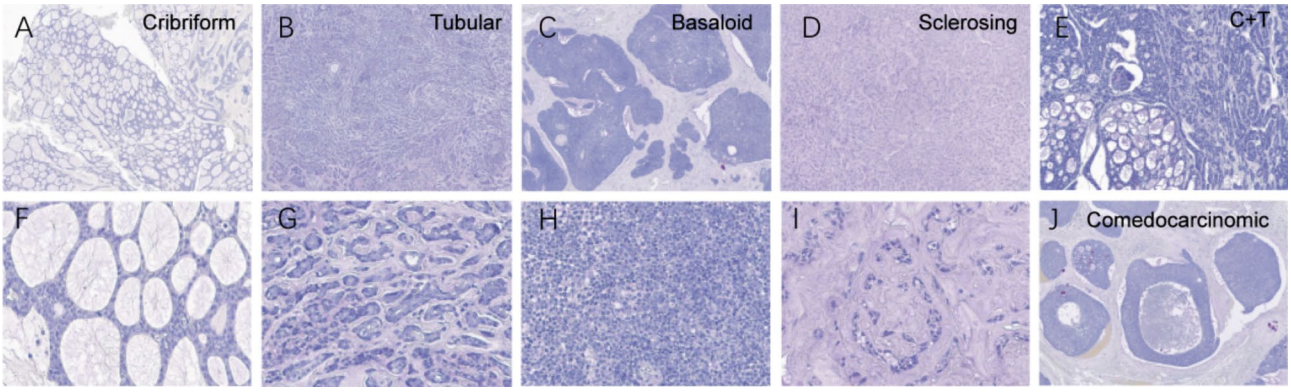

Fig. 1 Pathological pattern in LGACC. Cribriform (**A**, **F**), tubular (**B**, **G**), basaloid (**C**, **H**), sclerosing (**D**, **I**), cribriform + tubular (**E**), and comedocarcinoma (**J**). 4x magnification: A, B, C, D, E, J; 20x magnification: F, G, H, I

our study were diagnosed with T2 stages, we deleted the T4 stage patients on the following pathological subtype survival analysis. We further confirmed that, in LGACC patients diagnosed on T2 stage, the cribriform dominant pattern had a better prognosis than the non-cribriform dominant patients (Fig. 2D). In comparation, the basaloid dominant patients had a worse prognosis than the non-basaloid dominant patients (Fig. 2G) probably due to the different immune cell infiltration. Tubular and C + T dominant patients did not show significant differences in survival time compared with the non-dominant group (Fig. 2E and F). Due to the few patient numbers of sclerosing and comedocarcinoma subtypes, survival analysis was not performed. Our result indicated that the different pathological subtype configuration might indicate the prognosis on the tumors diagnosed on the same T stage.

CD45 expression in LGACC

CD45 expression was observed first to evaluate the immune cell infiltration in the whole sections of each tumor. The CD45 + immune cell infiltration varied among tumors. According to the density of CD45-positive cells, the tumor area was defined as "CD45 clustered" (Fig. 3A), "CD45 sparse", (Fig. 3B) and "CD45 non-infiltrated" (Fig. 3C) groups. The "CD45 non-infiltrated" area was defined as no positive immunostaining signal. The "CD45 sparse" area was defined as positive immunostaining cells distributing separately, with no clear border that could be delineated by the ImageJ software. The "CD45 sparse" area was defined as positive immunostaining cells with a clear border delineated by the ImageJ software. Cell nuclear count in sclerosing and comedocarcinoma patterns was scarce because of necrosis or stromal components, and CD45 expression could hardly be observed. Therefore, we did not include these patterns for further analysis. Moreover, all the patients in our study received en-bloc resection or orbital exenteration, so the tumor margin (TM) area between the mass and normal tissues could be observed. We noticed significant CD45-positive cells in the TM areas, which were included in further TIME analysis. The exact areas of different infiltration patterns in each pathological subtype were separately analyzed by ImageJ (Fig. 3D). As shown in Fig. 3E, the CD45 expression in most tumor areas was low. The cribriform had the highest overall CD45 + infiltration, and the TM area showed the second highest CD45 expression level. The basaloid had the lowest CD45 expression. The clustered type was hardly observed in the basaloid subtype. The tubular and C + T subtypes showed similar lymphocyte infiltration patterns.

Tumor immune microenvironment in LGACC

Due to the heterogeneous pathological constitution in individual LGACC tumor and diverse CD45 expressions in different pathological subtypes, we adopted the multiplex immunohistochemistry for spatial immune biomarker analysis to describe the TIME with geographic distribution information. According to the method developed by Tsujikawa et al. [25] and described in the Material and Method section, all the images were converted to grayscale and ascribed pseudo colors in ten channels (Fig. 4A). The immune cell lineages were designated by different combinations of biomarkers (Table 2; Fig. 5), The complexity of TIME in LGACC with geographic distribution was displayed in Fig. 4B.

To investigate the immune cell components in different pathological types as well as in TM areas (Fig. 6A), three sections were randomly picked in each tumor according to CD45 + cell infiltration. The immune cell densities and ratios were quantified by cytometry gating strategies and an unsupervised hierarchical clustering analysis was performed for subgroups. As shown in Fig. 6B, the TIME of LGACC of different pathological phenotypes was distinct. The number below the columns of Fig. 6B indicated the patient number, while the color of the number represented the pathological phenotypes. LGACC showed low immune cell infiltration in general. The immune cell panels tended to be clustered in consistency with the

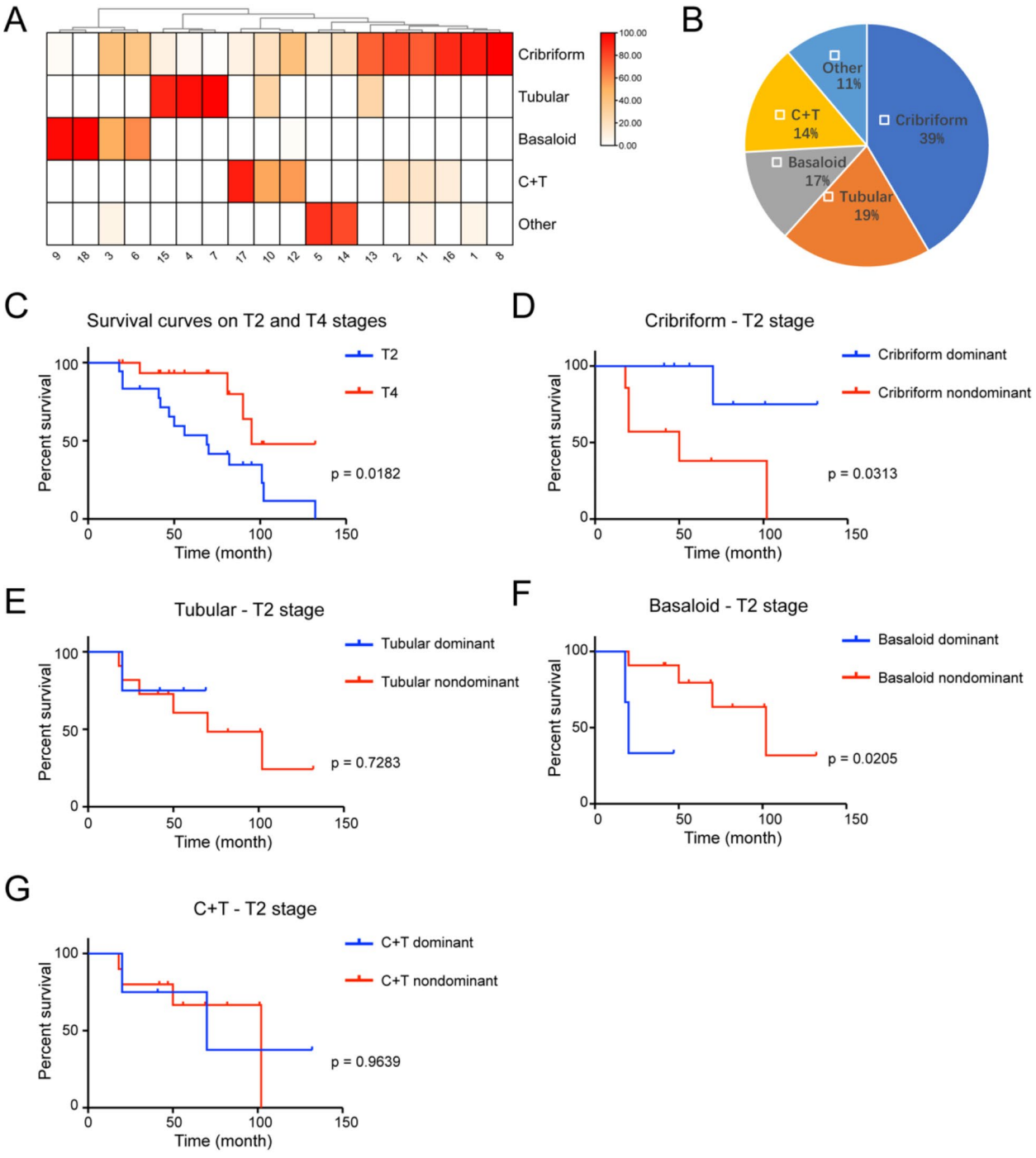

Fig. 2 Percentages of different pathological subtypes in LGACC and survival curve for specific type dominant patients. **A**: Mixture of pathological subtypes in individual tumors. Each column represented one individual. **B**: Percentages of each pathological subtypes overall. **C**: Significant survival curves between T2 stage patients (blue line) and T4 stage patients (red line) patients. **D**: Significant survival curves between cribriform dominant (blue line) and non-cribriform dominant (red line) patients diagnosed on T2 stage. **E**: Survival curves between tubular dominant (blue line) and non-tubular dominant (red line) patients diagnosed on T2 stage. **F**: Significant survival curves between basaloid dominant (blue line) and non-basaloid dominant (red line) patients diagnosed on T2 stage. **G**: Survival curves between C + T dominant (blue line) and non-C + T dominant (red line) patients diagnosed on T2 stage

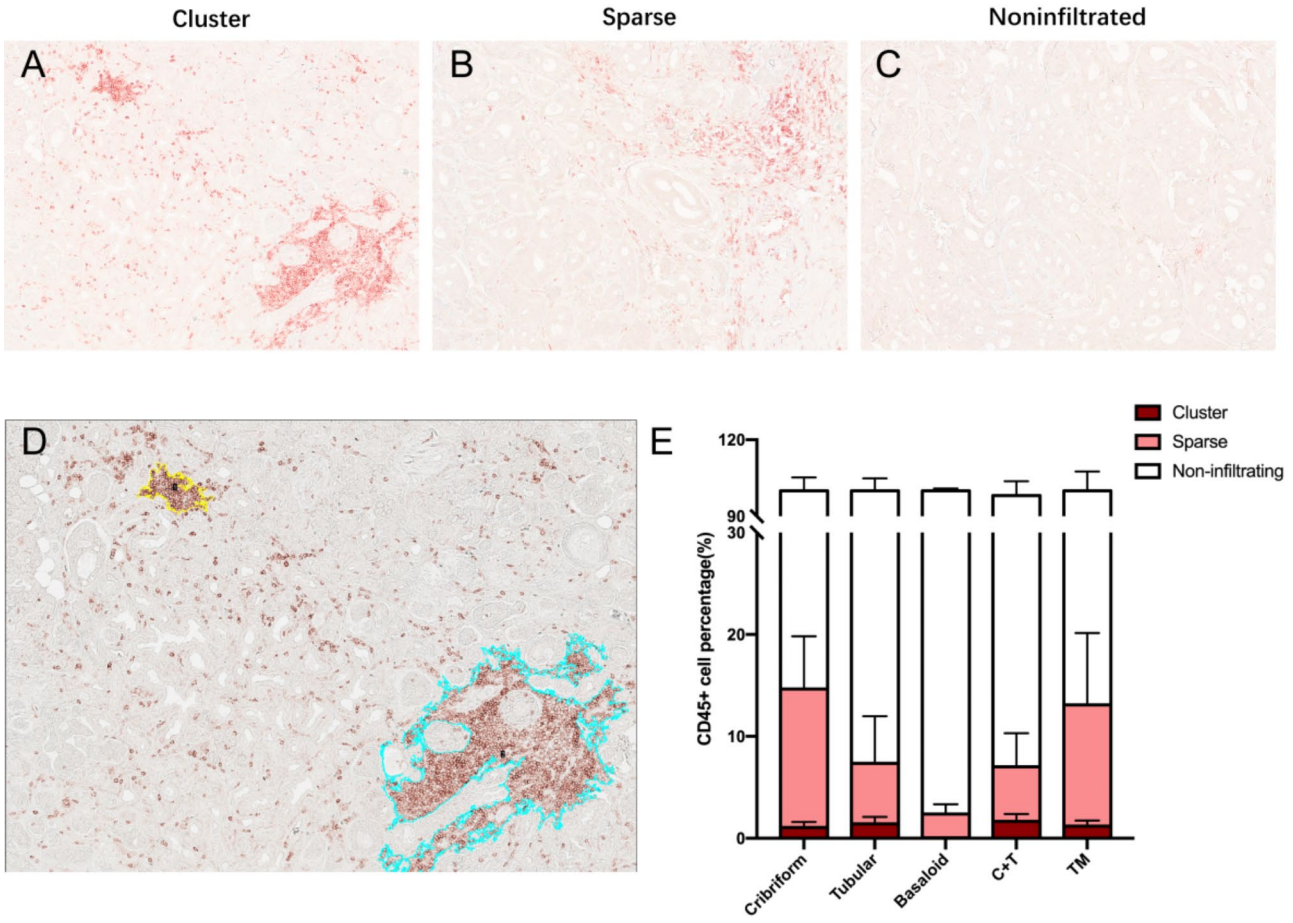

Fig. 3 Patterns of CD45 + cell infiltration in LGACC. **A**: Cluster distribution of CD45 + cells. **B**: Sparse distribution of CD45 + cells. **C**: Non-infiltration of CD45 + cells. **D**-**E**: Quantification of each pattern by ImageJ

pathological phenotypes instead of individuals. The cribriform and TM areas showed similarity in the immune cell panel. The CD8 + and CD4 + cells were the most abundant immune cells in the LGACC, majorly distributing in the TM and cribriform areas. The expression of PD-1 in CD4 + and CD8 + T cells was low. NK cells were barely seen in all pathological subtypes and TM areas. Treg and macrophage distribution could be observed in partial cribriform and TM areas. M2 macrophages took a more significant percentage as compared to the M1 macrophages. The percentages of individual immune cells was displayed in Fig. 6C. NK cells were the most abundant in the basaloid subtype (Fig. 7C). Other immune cells included in this study had more distribution in TM areas. For tumor areas, the cribriform subtype showed more immune cell infiltration than others (Fig. 7).

Discussion

LGACC is a very rare malignant disease, although it takes the biggest part in the malignancies originating from the lacrimal gland. It takes about 25% of all the ACCs from the head and neck [26]. Our study includes eighteen patients with full parts of pathological information. However, it was a small sample size for a comprehensive clinical retrospective study. More patients are still needed in future work, which will include more detailed descriptions on the TIME of the tumor with more advanced technologies like spatial transcriptomics, which will help us to unveil more information on this rare disease with poor prognosis under current clinical treatment modalities. Furthermore, as indicated by the result of our study, we should carry out clinical trials based on the immune cell infiltration difference, especially the CD8 + cell and macrophage subtype immunoregulation to develop immunotherapies and observe the clinical effect on different stages of LGACC.

Previous studies indicated that the risk factors related to poor diagnosis of ACC included the presence of the solid pathological pattern, MYB rearrangement high-grade transformation, perineural invasion, vascular dissemination, and nuclear atypia and [5, 7–9, 12]. The solid pathological pattern was proved to be associated with the worse clinical outcome [8, 9, 21, 24, 27]. However, ACC is characterized by heterogenous pathological subtypes.

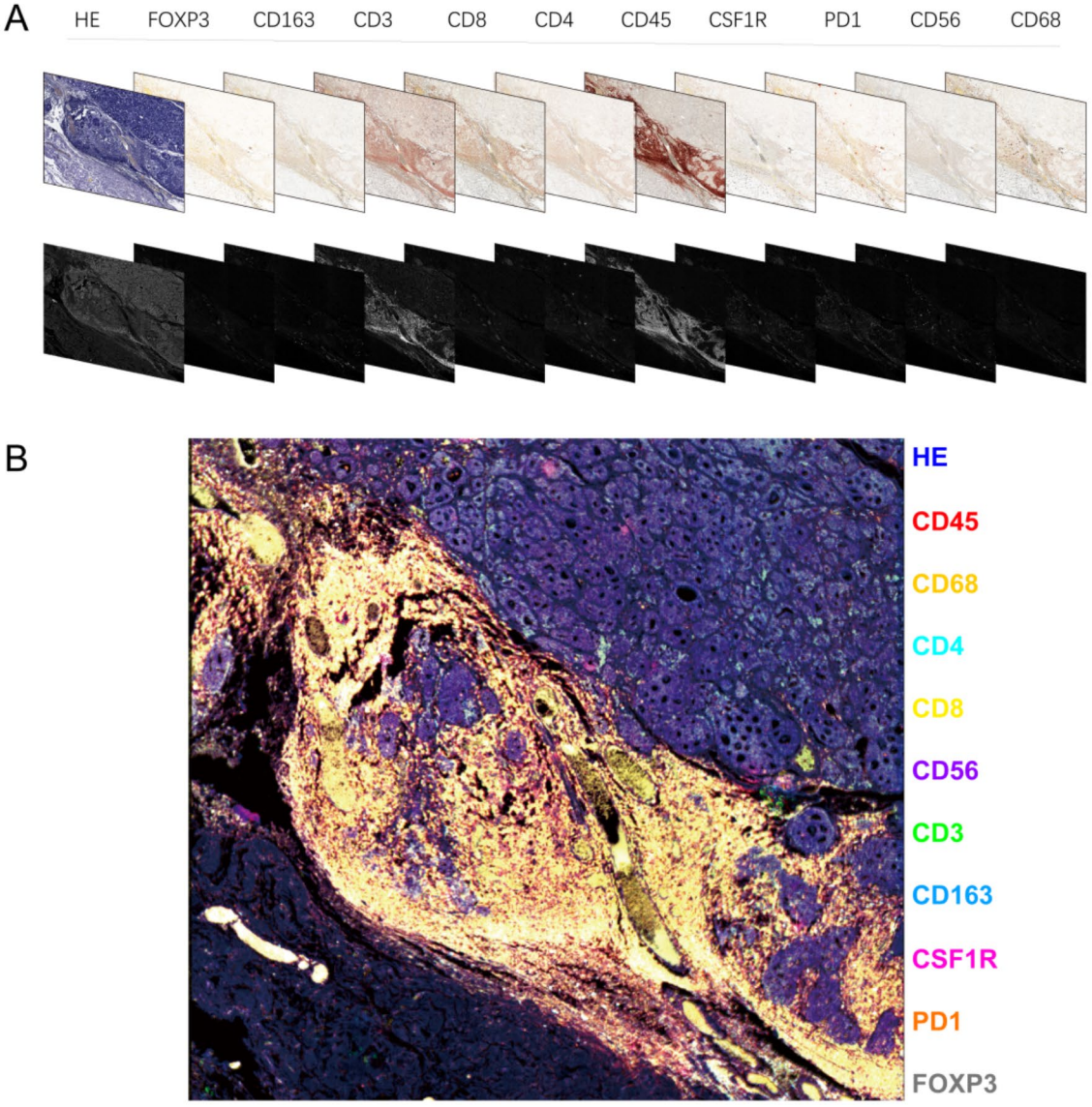

Fig. 4 TIME in LGACC. **A**: Working flow of multiplex immunohistochemistry and image processing of TIME. **B**: Constitution of TIME with geographic distribution in LGACC

Table 2 Immune cell lineage identification by biomarkers

CD4 + T cells	CD45 + CD3 + CD4+
CD4 + PD1 + T cell	CD45 + CD3 + CD4 + PD1+
CD8 + T cells	CD45 + CD3 + CD8+
CD8 + PD1 + T cell	CD45 + CD3 + CD8 + PD1+
Treg	CD45 + CD3 + CD4 + FOXP3+
NKs	CD45 + CD3-CD56+
M1TAM	CD45 + CSF1R + CD68 + CD163-
M2TAM	CD45 + CSF1R + CD68 + CD163+

Most previous studies described the tumor in a semi-quantitative way. It is the first study to analyze the exact pathological percentages of each subtype with nuclear in the whole scale of the tumor. We showed that the cribriform was the most common pathological subtype, consistent with previous reports on LGACC [8, 9]. However, in salivary ACC, cribriform was reported with varied percentages [28, 29]. The tubular type was the second typical phenotype in our study but the least seen in John et al. and David et al. reports on LGACC. The sclerosing and comedocarcinomas were the least common subtypes in our study, but in larger proportion in previous studies

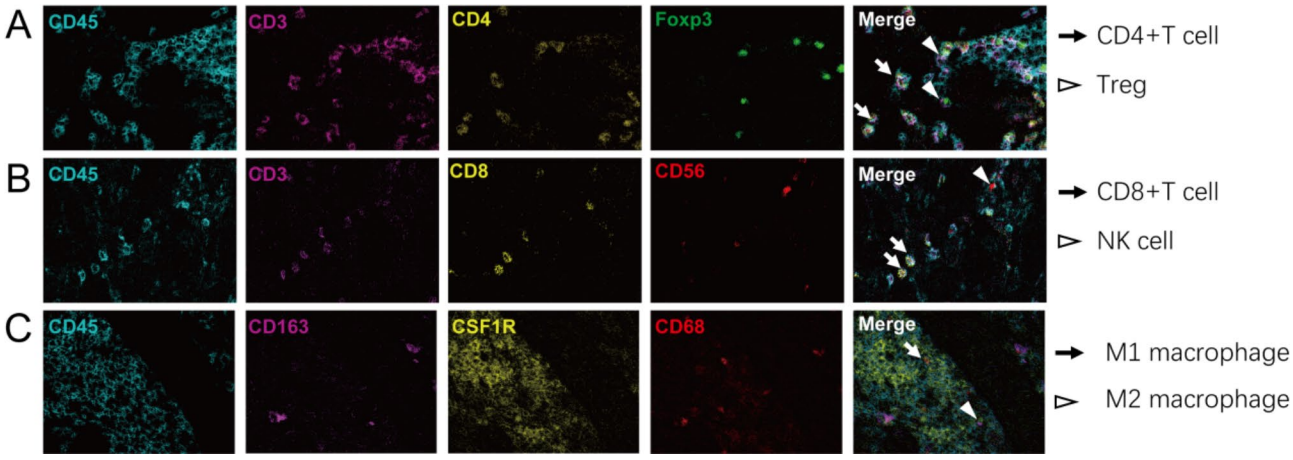

Fig. 5 Identification of specific immune cells in LGACC. **A**: CD4 + T cells (arrow) and Treg cell (arrowhead). **B**: CD8 + T cells (arrow) and NK cells (arrowhead). **C**: M1 macrophages cells (arrow) and M2 macrophages(arrowhead)

in LGACC [8, 9]. Similarly, the percentage of basaloid phenotype was different among the studies cited above. The consensus is that the basaloid presence and percentages are related to poor prognosis both in LGACC and salivary ACC, but the underlying mechanism needs to be further addressed.

There are multidisciplinary treatments for LGACC. Maximum surgical resection with adjuvant radiotherapy is considered in most patients. In current studies, both Proton and intra-arterial chemotherapy are proven to augment the outcomes [30–32]. However, despite multimodal approaches, this aggressive tumor still showed high dissemination potential, and once it happened, effective treatments were limited. Immunotherapy is one of the most promising new-generation cancer therapeutics, especially for patients in advanced stages. The complex interplay between tumor cells and the immune system is an essential determinant throughout tumor initiation, progression, and the response to therapies.

Most investigations on the immune microenvironment of ACC were conducted on salivary ACCs. Dou et al. reported 75 cases of ACC in the head and neck [21]. They adopted single-sample Gene Set Enrichment Analysis (ssGSEA) using bulk RNA-seq data. They showed that, compared with other cancer types, antigen-presenting machinery expression score and immune infiltration score were the lowest among ACC patients. Mosconi et al. investigated the immune marker expression level in 36 salivary ACC patients and indicated low immunogenicity and the expression of CD8 was low [24]. Doescher et al. [20] also confirmed the low immunogenicity in 50 salivary ACC patients, and only six patients exhibited the presence of tertiary lymphoid structures predominantly expressing CD8. Michaelides et al. [23] reported twelve salivary ACC patients with a significant elevation of macrophages with M2 polarization compared with normal salivary gland tissue, and CD4/CD8 quotient was heterogeneous in the tumor areas without relevant PD-L1 expression. Chen et al. [19] reported 24 salivary ACC patients, showing all patients were negative for PD-L1 expression. Only 16.7% of patients had focal high CD8 + cell infiltration, 33% with moderate infiltration, and 50% patients with low infiltration. Yang et al. [33] reported that the M2 macrophages were elevated in salivary ACC patients and associated with clinical progression and poor prognosis.

In our study, LGACC exhibited high heterogeneity. Most tumors were presented with multiple pathological subtypes with different percentages. Further investigation showed that tumor lymphocyte infiltration differed among different pathological subtypes. Therefore, spatial immune biomarker analysis with geographic distribution information is critical for TIME description. Consistent with previous studies on salivary ACCs, LGACC also showed low immune cell infiltration in the tumor areas but higher in the TM areas. In our study, eight types of immune cells were analyzed. Cytotoxic CD8 + T cells are proven to be the most potent effectors in anti-tumor immune responses and the immunotherapies [34]. In our study, CD8 + T cell showed high densities in the TM regions, indicating that immune reaction was aroused by the invasion of tumor cells into the normal tissue. The cribriform showed second abundant CD8 + T cells, and cribriform-dominant patients showed better clinical outcomes, probably due to the cytotoxic effect of CD8 + T cells to destroy the tumor cells. CD4 + T cells are a crucial component in developing and sustaining effective anti-tumor immunity. They also play critical functions in immunotherapies targeted in CD8 + T cell activation [35]. CD4 + T cells took the largest constitution of the immune cells investigated in our study, especially in the TM areas. Among the four pathological tumor subtypes, the percentage of CD4 + T cells was similar. PD-1 is expressed upon activation on CD4 + T cells, CD8 + T cells, B cells,

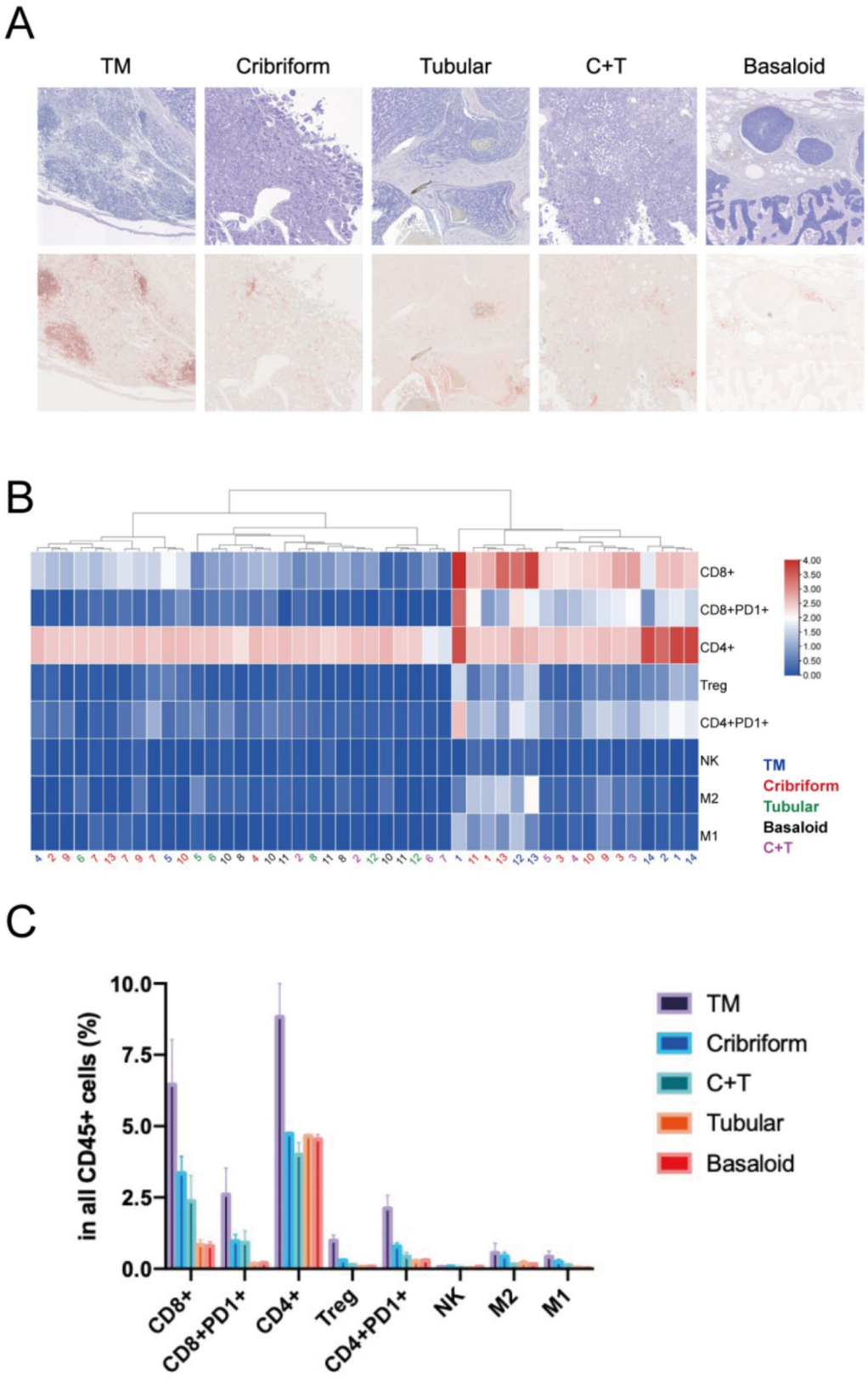

Fig. 6 TIME in different pathological subtypes in LGACC. **A**: CD45 + expression in each pathological subtype with 4x magnification. **B**: Heapmap of different immune cells in individual tumors. The number below the columns of Fig. 6B indicated the patient number, while the color of the number represented the pathological phenotypes. **C**: Percentages of different immune cells compared among pathological subtypes

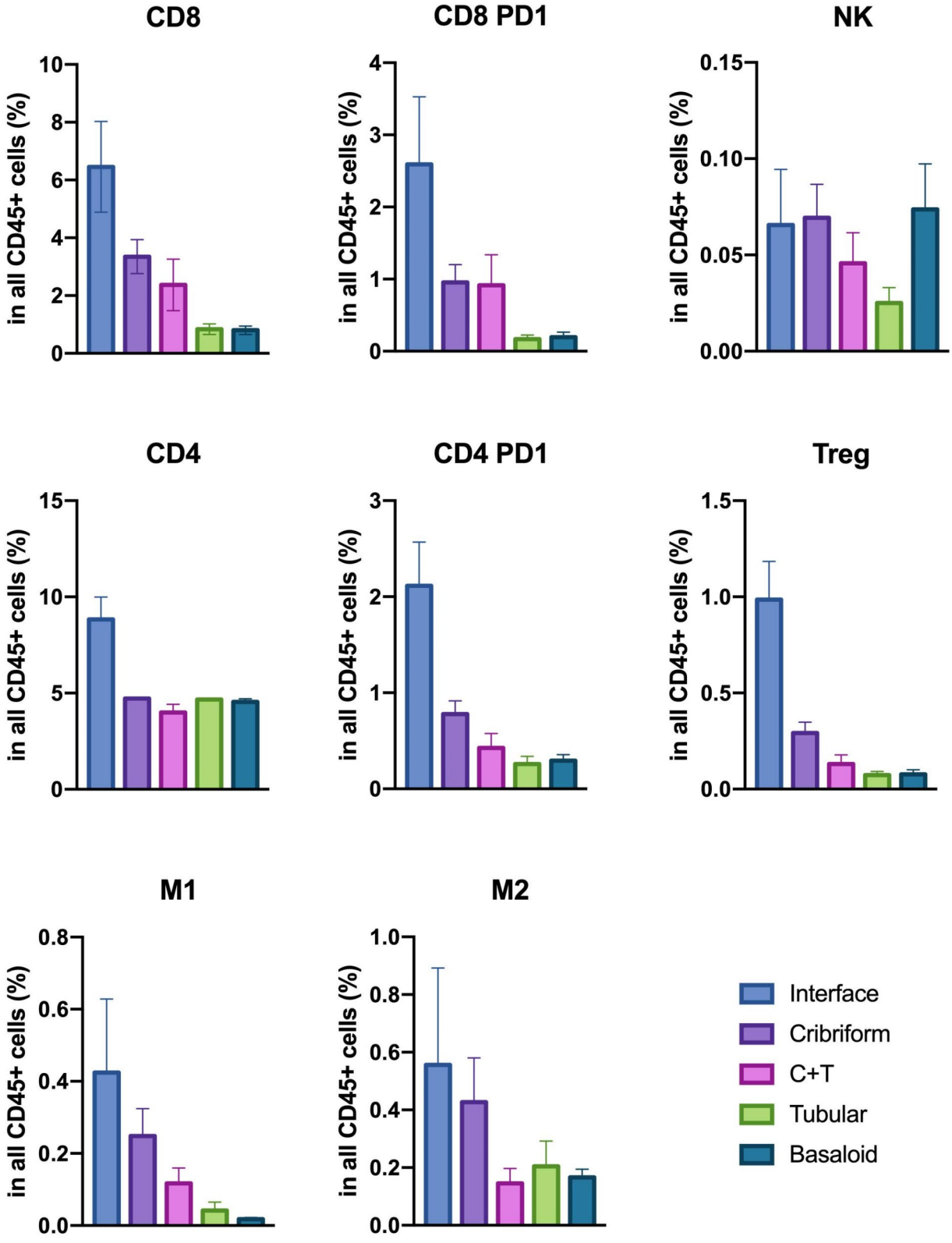

Fig. 7 Percentage of individual immune cell in different pathological subtypes in LGACC

natural killer T cells and monocytes. The PD-1 expression reflects T cell activation and plays a vital role in immunotherapies. In our study, tumors with cribriform and C + T subtypes possessed higher PD-1 CD8 + and CD4 + T cells than the tubular and basaloid subtypes. More regulatory mechanism needs to be further addressed, which could provide clues on immunotherapy designs. Tumor-associated macrophages (TAMs) are roughly divided into M1 and M2 subtypes, with different immune defense and tumor surveillance [36]. The two classes could transform into each other in response to the internal tumor environment. M2 TAM was reported to increase in salivary ACCs compared with the normal tissues and promote angiogenesis [23]. In our study, M2 TAMs also took a larger proportion than the M1 TAMs, especially in the basaloid subtype.

Our study depicted the percentages of pathological subtypes quantitatively in LGACC. A relationship between the cribriform/basaloid dominant type and prognosis was revealed. The TIME dissimilarities in different pathological subtypes could indicate the mechanism. We hope our study could provide an initial sketch of the TIME in LGACC, as well as novel therapeutic approaches.

Abbreviations

LGACC	lacrimal gland adenoid cystic carcinoma
TIME	tumor immune microenvironment

Supplementary Information

The online version contains supplementary material available at https://doi.org/10.1186/s12885-025-13438-z.

Supplementary Material 1

Acknowledgements

Not applicable.

Author contributions

Y.Z. and F.M. wrote the main manuscript text and prepared the figures; S.J. collected the clinical data; Y.B, R.C, R.Z and H. R performed the acquisition and interpretation of data; F.M. , Z. G. and J.Q. designed the work and substantively revised the main manuscript text.All authors reviewed the manuscript.

Funding

Supported by grants from the National Natural Science Foundation of China (Grant No. 81970835) and the Shanghai Committee of Science and Technology, China (Grant No.20Y11911200).

Data availability

The datasets used and/or analysed during the current study are available from the corresponding author on reasonable request.

Declarations

Ethics approval and consent to participate

This retrospective study was carried out in the Eye and ENT Hospital of Fudan University and approved by the ethics committee of this affiliation. The clinical and research conducts adhered to the tenets of the Declaration of Helsinki. All the patients in this study have signed informed consent of clinical data investigation for research purposes.

Consent for publication

Written informed consent for publication was obtained from all participants for the publication of this study and any accompanying materials.

Competing interests

The authors declare no competing interests.

Author details

[1]Department of Ophthalmology, Eye & ENT Hospital of Fudan University, Shanghai, China
[2]Laboratory of Myopia, Chinese Academy of Medical Sciences, Shanghai, China
[3]NHC Key Laboratory of Myopia, Fudan University, Shanghai, China
[4]Institute for Translational Brain Research, State Key Laboratory of Medical Neurobiology, MOE Frontiers Center for Brain Science, Fudan University, Shanghai, China
[5]Department of Pathology, Eye & ENT Hospital of Fudan University, Shanghai, China

Received: 15 October 2024 / Accepted: 3 January 2025
Published online: 31 March 2025

References

1. Bernardini FP, Devoto MH, Croxatto JO. Epithelial tumors of the lacrimal gland: an update. Curr Opin Ophthalmol. 2008;19(5):409–13.
2. Esmaeli B, Ahmadi MA, Youssef A, et al. Outcomes in patients with adenoid cystic carcinoma of the lacrimal gland. Ophthalmic Plast Reconstr Surg. 2004;20(1):22–6.
3. Karp JM, Gordon AJ, Hu K, et al. Pathologic features, treatment, and clinical outcomes of Lacrimal Gland Cancer. Cureus. 2023;15(8):e44466.
4. Moeyersoms AHM, Gallo RA, Zhang MG et al. Spatial Transcriptomics identifies expression signatures specific to lacrimal gland adenoid cystic carcinoma cells. Cancers (Basel) 2023; 15(12).
5. von Holstein SL, Fehr A, Persson M, et al. Adenoid cystic carcinoma of the lacrimal gland: MYB gene activation, genomic imbalances, and clinical characteristics. Ophthalmology. 2013;120(10):2130–8.
6. Le Tourneau C, Razak AR, Levy C, et al. Role of chemotherapy and molecularly targeted agents in the treatment of adenoid cystic carcinoma of the lacrimal gland. Br J Ophthalmol. 2011;95(11):1483–9.
7. Xu B, Drill E, Ho A, et al. Predictors of Outcome in Adenoid cystic carcinoma of salivary glands: a clinicopathologic study with correlation between MYB Fusion and protein expression. Am J Surg Pathol. 2017;41(10):1422–32.
8. Lee DA, Campbell RJ, Waller RR, Ilstrup DM. A clinicopathologic study of primary adenoid cystic carcinoma of the lacrimal gland. Ophthalmology. 1985;92(1):128–34.
9. Gamel JW, Font RL. Adenoid cystic carcinoma of the lacrimal gland: the clinical significance of a basaloid histologic pattern. Hum Pathol. 1982;13(3):219–25.
10. Szanto PA, Luna MA, Tortoledo ME, White RA. Histologic grading of adenoid cystic carcinoma of the salivary glands. Cancer. 1984;54(6):1062–9.
11. van Weert S, van der Waal I, Witte BI, Leemans CR, Bloemena E. Histopathological grading of adenoid cystic carcinoma of the head and neck: analysis of currently used grading systems and proposal for a simplified grading scheme. Oral Oncol. 2015;51(1):71–6.
12. Chen TY, Keeney MG, Chintakuntlawar AV, et al. Adenoid cystic carcinoma of the lacrimal gland is frequently characterized by MYB rearrangement. Eye (Lond). 2017;31(5):720–5.
13. Binnewies M, Roberts EW, Kersten K, et al. Understanding the tumor immune microenvironment (TIME) for effective therapy. Nat Med. 2018;24(5):541–50.
14. Chen DS, Mellman I. Oncology meets immunology: the cancer-immunity cycle. Immunity. 2013;39(1):1–10.
15. Khong HT, Restifo NP. Natural selection of tumor variants in the generation of tumor escape phenotypes. Nat Immunol. 2002;3(11):999–1005.
16. Lv B, Wang Y, Ma D, et al. Immunotherapy: reshape the Tumor Immune Microenvironment. Front Immunol. 2022;13:844142.
17. Drake CG, Jaffee E, Pardoll DM. Mechanisms of immune evasion by tumors. Adv Immunol. 2006;90:51–81.
18. Thomas DA, Massague J. TGF-beta directly targets cytotoxic T cell functions during tumor evasion of immune surveillance. Cancer Cell. 2005;8(5):369–80.

19. Chen W, Fung AS, McIntyre JB, et al. Assessment of Tumour infiltrating lymphocytes and Pd-l1 expression in adenoid cystic carcinoma of the salivary gland. Clin Invest Med. 2021;44(1):E38–41.
20. Doescher J, Meyer M, Arolt C et al. Patterns of Tumor infiltrating lymphocytes in adenoid cystic carcinoma of the Head and Neck. Cancers (Basel) 2022; 14(6).
21. Dou S, Li R, He N, et al. The Immune Landscape of Chinese Head and Neck Adenoid Cystic Carcinoma and clinical implication. Front Immunol. 2021;12:618367.
22. Linxweiler M, Kuo F, Katabi N, et al. The Immune Microenvironment and Neoantigen Landscape of Aggressive Salivary Gland carcinomas Differ by Subtype. Clin Cancer Res. 2020;26(12):2859–70.
23. Michaelides I, Kunzel J, Ettl T, et al. Adenoid cystic carcinoma of the salivary glands: a pilot study of potential therapeutic targets and characterization of the immunological tumor environment and angiogenesis. Eur Arch Otorhinolaryngol. 2023;280(6):2937–44.
24. Mosconi C, de Arruda JAA, de Farias ACR, et al. Immune microenvironment and evasion mechanisms in adenoid cystic carcinomas of salivary glands. Oral Oncol. 2019;88:95–101.
25. Tsujikawa T, Kumar S, Borkar RN, et al. Quantitative multiplex immunohistochemistry reveals myeloid-inflamed Tumor-Immune Complexity Associated with Poor Prognosis. Cell Rep. 2017;19(1):203–17.
26. Friedrich RE, Bleckmann V. Adenoid cystic carcinoma of salivary and lacrimal gland origin: localization, classification, clinical pathological correlation, treatment results and long-term follow-up control in 84 patients. Anticancer Res. 2003;23(2A):931–40.
27. Ben Salha I, Bhide S, Mourtzoukou D, Fisher C, Thway K. Solid variant of adenoid cystic carcinoma: difficulties in Diagnostic Recognition. Int J Surg Pathol. 2016;24(5):419–24.
28. Moskaluk CA. Adenoid cystic carcinoma: clinical and molecular features. Head Neck Pathol. 2013;7(1):17–22.
29. Belulescu IC, Margaritescu C, Dumitrescu CI, Munteanu LDA, Margaritescu C. Adenoid cystic carcinoma of salivary gland: a ten-year single Institute experience. Curr Health Sci J. 2020;46(1):56–65.
30. Tse DT, Benedetto P, Dubovy S, Schiffman JC, Feuer WJ. Clinical analysis of the effect of intraarterial cytoreductive chemotherapy in the treatment of lacrimal gland adenoid cystic carcinoma. Am J Ophthalmol. 2006;141(1):44–53.
31. Tse DT, Benedetto PW, Tse BC, Feuer WJ. Neoadjuvant intra-arterial cytoreductive chemotherapy for lacrimal gland adenoid cystic carcinoma: a long-term follow-up study of a Trimodal Strategy. Am J Ophthalmol. 2022;240:239–51.
32. Maniar A, Saqi A, Troob SH, et al. Targeted neoadjuvant intra-arterial chemotherapy in Lacrimal Gland Adenoid cystic carcinoma: a histological correlation using apoptotic tumor markers. Ophthalmic Plast Reconstr Surg. 2022;38(1):e28–33.
33. Yang Z, Li H, Wang W, et al. CCL2/CCR2 Axis promotes the progression of salivary adenoid cystic carcinoma via recruiting and reprogramming the Tumor-Associated macrophages. Front Oncol. 2019;9:231.
34. Raskov H, Orhan A, Christensen JP, Gogenur I. Cytotoxic CD8(+) T cells in cancer and cancer immunotherapy. Br J Cancer. 2021;124(2):359–67.
35. Tay RE, Richardson EK, Toh HC. Revisiting the role of CD4(+) T cells in cancer immunotherapy-new insights into old paradigms. Cancer Gene Ther. 2021;28(1–2):5–17.
36. Zhou J, Tang Z, Gao S, Li C, Feng Y, Zhou X. Tumor-Associated macrophages: recent insights and therapies. Front Oncol. 2020;10:188.

Publisher's note